Structural Engineering and Mechanics, *Vol. 67, No. 2 (2018) 143-153*
DOI: https://doi.org/10.12989/sem.2018.67.2.143

Surface and flexoelectricity effects on size-dependent thermal stability analysis of smart piezoelectric nanoplates

Farzad Ebrahimi* and Mohammad Reza Barati

Department of Mechanical Engineering, Faculty of Engineering, Imam Khomeini International University, P.O.B. 16818-34149, Qazvin, Iran

(Received May 6, 2018, Revised May 2, 2018, Accepted May 3, 2018)

Abstract. Thermal buckling of nonlocal flexoelectric nanoplates incorporating surface effects is analyzed for the first time. Coupling of strain gradients and electrical polarizations is introduced by flexoelectricity. It is assumed that flexoelectric nanoplate is subjected to uniform and linear temperature distributions. Long range interaction between atoms of nanoplate is modeled via nonlocal elasticity theory. The residual surface stresses which are usually neglected in modeling of flexoelectric nanoplates are incorporated into nonlocal elasticity to provide better understanding of the physic of problem. A Galerkin-based approach is implemented to solve the governing equations derived from Hamilton's principle are solved. The verification of obtained results is performed by comparing buckling loads of flexoelectric nanoplate with previous data. It is shown that buckling loads of flexoelectric nanoplate are significantly affected by thermal loading type, temperature change, nonlocal parameter, surface effect, plate thickness and boundary conditions.

Keywords: thermal buckling; flexoelectric nanoplate; surface effect; nonlocal elasticity theory

1. Introduction

Small scale plates are the basic structures used in several applications such as nano-electro-mechanical systems, nano-probes, atomic force microscope (AFM), nanoactuators and nanosensors. At nano scale, the physical and mechanical properties of small scale structures render evident size effects, which are quite different from their bulk counterparts.

As the size dependent behaviors have been experimentally observed in small-scale structures, exploring the size effects on the mechanical characteristics of such nanostructures has motivated the scientific community in recent years (Ebrahimi and Barati 2016a, b, c, d, e, f, g, h, i, j, k, l, m, n). Since the models based on classical continuum mechanics are not capable of describing such size dependent behaviors in nano-scale elements, several nonclassical continuum theories such as the nonlocal, strain gradient and couple stress theories that contain additional material length scale parameters have been developed to capture the size effect (Ebrahimi and Barati 2017). Also, thermal buckling and free vibration analysis of nanobeams subjected to temperature distribution have been exactly investigated by Ebrahimi and Salari (2015a, b, c) and Ebrahimi *et al.* (2015a, b). Ebrahimi and Barati (2016o, p, q) investigated buckling behavior of smart piezoelectrically actuated higher-order size-dependent graded nanoscale beams and plates in thermal environment.

The flexoelectricity is related to a particular electromechanical coupling phenomenon between polarization and strain gradients (Jiang *et al.* 2013). In fact, imposing a strain gradient to dielectrics can induce an electrical polarization by breaking the inversion symmetry. It is well known that the flexoelectricity provides an inherent size effect as the dimensions of nanostructured materials decrease. Contrary to flexoelectricity, the piezoelasticity cannot introduce such size effect for a wide range of dielectrics applied in NEMs. Also, having a large ratio of surface area to volume in nanomaterials, surface effects have been believed to involve the size-dependency of material properties. According to the surface elasticity theory developed by Gurtin and Murdoch (1975), the size-dependency of nanoscale structures due to the surface effects have been broadly researched by the modified continuum models from static and dynamic perspectives (Wang and Wang 2011, Ebrahimi and Boreiry 2015, Ebrahimi *et al.* 2016, Hosseini *et al.* 2016).

Recently, a number of researches are performed to incorporate the surface effects in analysis of piezoelectric nanostructure. Yan and Jiang (2011) investigated surface effects on vibration and buckling of piezoelectric nanobeams with surface effects. Also, Yan and Jiang (2012) explored vibrational and stability behaviors of piezoelectric nanoplates considering surface effects and in-plane constraints. A Two-dimensional theory of surface piezoelasticity of plates is presented by Zhang *et al.* (2013). Also, Zhang *et al.* (2014a) researched wave propagation of piezoelectric nanoplates considering surface effects. Also, Zhang *et al.* (2014b) investigated the influence of surface piezoelasticity on the buckling behavior of piezoelectric nanofilms subjected to mechanical loadings. Recently, Li and Pan (2016) presented bending analysis of a sinusoidal piezoelectric nanoplate with surface effects. As a deficiency, the nonlocality of stress field is not considered in these papers. Recently, modeling of nanostructures by using the nonlocal elastic field theory of Eringen (1972, 1983) has received wide importance. The

*Corresponding author, Ph.D.
E-mail: febrahimy@eng.ikiu.ac.ir

ISSN: 1225-4568 (Print), 1598-6217 (Online)

prominence of nonlocal theory of elasticity has stimulated the researchers to investigate the behavior of the nanostructures much accurately (Li *et al.* 2016). This theory contains a nonlocal stress field parameter which introduces a stiffness-softening influence on the nanostructures (Ebrahimi and Barati 2016a, b, Ebrahimi *et al.* 2016).

To include the nonlocal effects in analysis of piezoelectric nanostructures, Ke and Wang (2012) investigated thermal vibration of piezoelectric nanoscale beams according to the nonlocal theory.

Wang and Wang (2012) researched the electromechanical coupling behavior of a piezoelectric nanowire incorporating both surface and nonlocal effects. Also, Liu *et al.* (2013) presented vibration analysis of piezoelectric nanoplates exposed to thermo-electro-mechanical loads based on the nonlocal theory. Asemi *et al.* (2014) explored the Influence of initial stress on vibrational behavior of double-piezoelectric-nanoplate systems under different boundary conditions. Zang *et al.* (2014) investigated axial wave propagation of piezoelectric nanoplates considering surface and nonlocal effects. Liu *et al.* (2014) studied buckling and post-buckling behaviors of piezoelectric Timoshenko nanobeams under thermo-electro-mechanical loadings. Ke *et al.* (2015) reported vibration response of a nonlocal piezoelectric nanoplate considering various boundary conditions. Liu *et al.* (2015) presented large amplitude vibration of nonlocal piezoelectric nanoplates under electro-mechanical coupling. Asemi *et al.* (2015) researched the nanoscale mass detection using vibrating piezoelectric ultrathin films subjected to thermo-electro-mechanical loads. Ansari *et al.* (2016) presented thermo-electrical vibrational analysis of post-buckled piezoelectric nanosize beams according to the nonlocal elasticity theory. Ebrahimi and Barati (2016c, d) investigated dynamic behavior of non-homogenous piezoelectric nanobeams under magnetic field. Wang *et al.* (2016) investigated vibration response of piezoelectric circular nanoplates considering surface and nonlocal effects. Ebrahimi and Barati (2016e) presented buckling analysis of nonlocal third-order shear deformable piezoelectric nanobeams embedded in elastic medium. Ebrahimi and Barati (2016f) studied buckling behavior of smart higher order piezoelectric functionally graded nanosize beams subjected to the electro-magnetic field. Liu *et al.* (2016) studied nonlinear vibration of piezoelectric nanoplates using nonlocal Mindlin plate theory.

A number of papers have been recently published to consider flexoelectric effect in analysis of piezoelectric nanostructures. Zhang *et al.* (2014) examined the flexoelectric effect on the electroelastic and vibration responses of piezoelectric nanoplates. Liang *et al.* (2014) showed the influences of surface and flexoelectricity on a piezoelectric nanobeam. Zhang and Jiang (2014) investigated bending behavior of piezoelectric nanoplates due to surface effects and flexoelectricity. Yang *et al.* (2015) examined electromechanical behavior of piezoelectric nanoplates with flexoelectricity under simply-supported boundary conditions. Liang *et al.* (2015) presented buckling and vibration behaviors of piezoelectric nanowires due to flexoelectricity. It is clear that buckling analysis of flexoelectric nanoplates is very rare in the literature. Only in one paper, Liang *et al.* (2016) examined buckling and vibration of flexoelectric nanofilms under simply-supported boundary conditions. But, they did not consider the effects of surface piezoelasticity, nonlocality and other kinds of boundary conditions in their model.

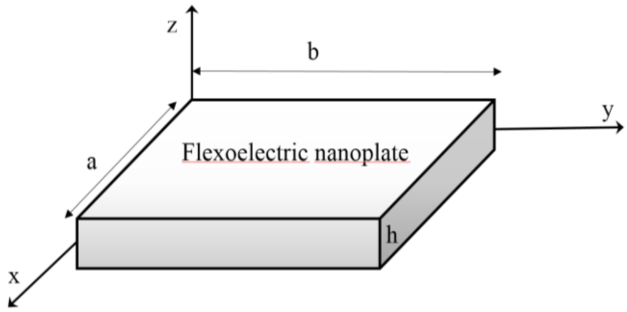

Fig. 1 Geometry and coordinates of flexoelectric nanoplate

In fact, literature survey indicates that none of previous papers on flexoelectric nanoplates have not considered nonlocal effects in their analysis. It is reported that the mechanical behavior of piezoelectric nanoplates is significantly influenced by the presence of nonlocality. Therefore, there is a strong scientific need to investigate buckling behavior of flexoelectric nanoplates incorporating both surface piezoelasticity and nonlocal effects.

This paper deals with thermo-mechanical buckling behavior of flexoelectric nanoplates under uniform and linear temperature distributions. Flexoelectric nanoplates can tolerate higher buckling loads compared with conventional piezoelectric nanoplates, especially at lower thicknesses. Both nonlocal and surface effects are considered in the analysis of flexoelectric nanoplates for the first time. Hamilton's principle is employed to derive the governing equations and the related boundary conditions which are solved applying a Galerkin-based solution. Comparison study is also performed to verify the present formulation with those of previous data. Numerical results are presented to investigate the influences of the flexoelectricity, nonlocal parameter, surface elasticity, temperature rise, plate thickness and various boundary conditions on the critical buckling load of thermally affected flexoelectric nanoplate.

2. Nonlocal elasticity theory for the piezoelectric materials with flexoelectric effect

Suppose a nanoplate made of PZT-5H piezoelectric material, as shown in Fig. 1. According to the nonlocal elasticity model (Eringen 1972) which contains wide range interactions between points in a continuum solid, the stress state at a point inside a body is introduced as a function of the strains of all neighbor points. The influence of flexoelectricity due to the elastic polarization P_i induced by strain gradient, and the elastic stress created by electric field gradient, can be expressed by (Li and Pan 2016)

$$\sigma_{ij} - (e_0 a)^2 \nabla^2 \sigma_{ij} = C_{ijkl}\varepsilon_{kl} - e_{kij}E_k + f_{klij}\frac{\partial E_k}{\partial x_l} - C_{ijkl}\alpha_{kl}\Delta T \tag{1a}$$

$$P_i - (e_0 a)^2 \nabla^2 P_i = \varepsilon_0 \chi_{ij} E_j + e_{ikl}\varepsilon_{kl} + f_{ijkl}\frac{\partial \varepsilon_{kl}}{\partial x_j} - p_i \Delta T \tag{1b}$$

where σ_{ij}, ε_{ij}, E_k denote the stress, strain and electric field components, respectively; C_{ijkl}, e_{kij} and k_{ik} are elastic, piezoelectric and dielectric constant, respectively. Also, χ_{ij} is the relative dielectric susceptibility and f_{ijkl} is the flexoelectric coefficient. α_{kl}, ΔT and p_i are thermal expansion coefficient, temperature change and pyroelectric constant, respectively.

Also, $e_0 a$ is nonlocal parameter which is introduced to describe the size-dependency of nanostructures. The effect of flexoelectricity is involved using the following expression of the electric enthalpy energy density was as follows

$$H=-\frac{1}{2}a_{kl}E_kE_l+\frac{1}{2}c_{ijkl}\varepsilon_{ij}\varepsilon_{kl}-e_{kij}E_k\varepsilon_{ij}-\frac{1}{2}f_{klij}(E_k\frac{\partial\varepsilon_{ij}}{\partial x_l}-\varepsilon_{ij}\frac{\partial E_k}{\partial x_l}) \tag{2}$$

Finally, the constitutive relations incorporating nonlocal and flexoelectricity effects can be expressed by

$$(1-(e_0\,a)^2\nabla^2)\sigma_{ij}=\frac{\partial H}{\partial\varepsilon_{ij}}=C_{ijkl}\varepsilon_{kl}-e_{kij}E_k+\frac{f_{klij}}{2}\frac{\partial E_k}{\partial x_l} \tag{3a}$$

$$(1-(e_0\,a)^2\nabla^2)\tau_{ijl}=\frac{\partial H}{\partial(\partial\varepsilon_{ij}/\partial x_l)}=-f_{ijkl}E_k \tag{3b}$$

$$(1-(e_0\,a)^2\nabla^2)D_i=-\frac{\partial H}{\partial E_i}=a_{ij}E_j+e_{ikl}\varepsilon_{kl}+\frac{f_{ijkl}}{2}\frac{\partial\varepsilon_{kl}}{\partial x_j} \tag{3c}$$

$$(1-(e_0\,a)^2\nabla^2)Q_{ij}=\frac{\partial H}{\partial(\partial E_i/\partial x_j)}=-\frac{f_{ijkl}}{2}\varepsilon_{kl} \tag{3d}$$

in which τ_{ijl} denotes the moment stress tensor due to the converse flexoelectric effect, D_i is the electric displacement vector and Q_{ij} denotes the electric quadrupole density due to flexoelectricity, respectively. The size-dependent phenomena in piezoelectric nanostructures due to flexoelectricity involved in Eq. (3) is reported in analysis of nanowires, nanobeams and nanoplates. Taking into account the surface effects, i.e., the residual surface stress, the surface elasticity, and the surface piezoelectricity, the surface internal energy density U_s can be defined by the surface strain and the surface polarization as

$$U_s=\Gamma_{\alpha\beta}\varepsilon^s_{\alpha\beta}-\frac{1}{2}a^s_{\gamma\kappa}E^s_\gamma E^s_\kappa+\frac{1}{2}c^s_{\alpha\beta\gamma\kappa}\varepsilon^s_{\alpha\beta}\varepsilon^s_{\gamma\kappa}-e^s_{\kappa\alpha\beta}E^s_\kappa\varepsilon^s_{\alpha\beta} \tag{4}$$

in which $\Gamma_{\alpha\beta}$ denotes the surface residual stress tensor, $a^s_{\gamma\kappa}$ and $c^s_{\alpha\beta\gamma\kappa}$ denote the surface permittivity and surface elastic constants. Also, $e^s_{\kappa\alpha\beta}$ and E^s_κ are the surface piezoelectric tensor and surface electric field. Finally, the nonlocal surface constitutive relations can be written as

$$(1-(e_0\,a)^2\nabla^2)\sigma^s_{\alpha\beta}=\frac{\partial U_s}{\partial\varepsilon_{\alpha\beta}}=\Gamma_{\alpha\beta}+c^s_{\alpha\beta\gamma\kappa}\varepsilon^s_{\gamma\kappa}-e^s_{\kappa\alpha\beta}E^s_\kappa \tag{5a}$$

$$(1-(e_0\,a)^2\nabla^2)D^s_\gamma=-\frac{\partial U_s}{\partial E^s_\gamma}=a^s_{\gamma\kappa}E^s_\kappa+e^s_{\gamma\alpha\beta}\varepsilon^s_{\alpha\beta} \tag{5b}$$

where $\sigma^s_{\alpha\beta}$ and D^s_γ are the surface Cauchy stress and surface electric displacement.

3. Theoretical formulation

Here, the classical plate theory is employed for modeling of a piezoelectric nanoplate with surface, nonlocal and flexoelectric effects. The displacement field at any point of the nanoplate can be written as

$$u_1(x,y,z)=u-z\frac{\partial w}{\partial x} \tag{6a}$$

$$u_2(x,y,z)=v-z\frac{\partial w}{\partial y} \tag{6b}$$

$$u_3(x,y,z)=w \tag{6c}$$

where u and v are displacements of the mid-surface and w is the bending displacement, respectively. Nonzero strains and strain-gradients of the present plate model are expressed as

$$\begin{aligned}
&\varepsilon_{xx}=\frac{\partial u_1}{\partial x}=\frac{\partial u}{\partial x}-z\frac{\partial^2 w}{\partial x^2},\quad \varepsilon_{yy}=\frac{\partial u_2}{\partial y}=\frac{\partial v}{\partial y}-z\frac{\partial^2 w}{\partial y^2}\\
&\gamma_{xy}=\frac{\partial u_1}{\partial y}+\frac{\partial u_2}{\partial x}=\frac{\partial u}{\partial y}+\frac{\partial v}{\partial x}-2z\frac{\partial^2 w}{\partial x\partial y}\\
&\eta_{xxz}=\frac{\partial\varepsilon_{xx}}{\partial z}=-\frac{\partial^2 w}{\partial x^2},\quad \eta_{yyz}=\frac{\partial\varepsilon_{yy}}{\partial z}=-\frac{\partial^2 w}{\partial y^2}\\
&\eta_{xyz}=\frac{\partial\gamma_{xy}}{\partial z}=-2\frac{\partial^2 w}{\partial x\partial y}
\end{aligned} \tag{7}$$

Through extended Hamilton's principle, the governing equations can be derived as follows

$$\int_0^t\delta(\Pi_S+\Pi_W)\,dt=0 \tag{8}$$

where Π_S and Π_W are strain energy and external forces work. The strain energy can be written as

$$\begin{aligned}
\delta\Pi_S=&\int_v(\sigma_{xx}\delta\varepsilon_{xx}+\sigma_{yy}\delta\varepsilon_{yy}+\sigma_{xy}\delta\gamma_{xy}+\tau_{xxz}\eta_{xxz}+\tau_{yyz}\eta_{yyz}+\tau_{xyz}\eta_{xyz})\,dV\\
&+\int_S(\sigma^s_{xx}\delta\varepsilon_{xx}+\sigma^s_{yy}\delta\varepsilon_{yy}+\sigma^s_{xy}\delta\gamma_{xy})\,dS
\end{aligned} \tag{9a}$$

Substituting Eqs. (15) and (16) into Eq.(18) yields

$$\begin{aligned}
\delta\Pi_S=&\int_0^a\int_0^b[(N_{xx}+N^s_{xx})\frac{\partial\delta u}{\partial x}-(M_{xx}+M^s_{xx})\frac{\partial^2\delta w}{\partial x^2}+(N_{yy}+N^s_{yy})\frac{\partial\delta v}{\partial y}-(M_{yy}+M^s_{yy})\frac{\partial^2\delta w}{\partial y^2}\\
&+(N_{xy}+N^s_{xy})(\frac{\partial\delta u}{\partial y}+\frac{\partial\delta v}{\partial x})-2(M_{xy}+M^s_{xy})\frac{\partial^2\delta w}{\partial x\partial y}+P_{xxz}\frac{\partial^2\delta w}{\partial x^2}+P_{yyz}\frac{\partial^2\delta w}{\partial y^2}]dxdy
\end{aligned} \tag{9b}$$

in which the variables introduced in arriving at the last expression are defined as follows

$$\begin{aligned}
&(N_i,M_i)=\int_A(1,z)\sigma_i\,dA,\ i=(x,y,xy)\\
&P_i=\int_A\tau_i\,dA,\ i=(xxz,yyz)
\end{aligned} \tag{10}$$

The work done by applied forces can be written in the form

$$\delta\Pi_W=\int_0^a\int_0^b(N_x^0\frac{\partial w}{\partial x}\frac{\partial\delta w}{\partial x}+N_y^0\frac{\partial w}{\partial y}\frac{\partial\delta w}{\partial y}+2\delta N_{xy}^0\frac{\partial w}{\partial x}\frac{\partial w}{\partial y})dxdy \tag{11}$$

where N_x^0, N_y^0, N_{xy}^0 are in-plane applied loads. The following Euler-Lagrange equations are obtained by inserting Eqs. (9b) and (11) in Eq. (8) when the coefficients of δu, δv, δw are equal to zero

$$\frac{\partial(N_{xx}+N_{xx}^s)}{\partial x}+\frac{\partial(N_{xy}+N_{xy}^s)}{\partial y}=0 \tag{12a}$$

$$\frac{\partial(N_{xy}+N_{xy}^s)}{\partial x}+\frac{\partial(N_{yy}+N_{yy}^s)}{\partial y}=0 \tag{12b}$$

$$\begin{aligned}&\frac{\partial^2(M_{xx}+M_{xx}^s)}{\partial x^2}+2\frac{\partial^2(M_{xy}+M_{xy}^s)}{\partial x\partial y}+\frac{\partial^2(M_y+M_y^s)}{\partial y^2}+\frac{\partial^2 P_{xxz}}{\partial x^2}+\frac{\partial^2 P_{yyz}}{\partial y^2}\\&-b(N^T+N^0)\nabla^2 w+2b\sigma_0\nabla^2 w=0\end{aligned} \tag{12c}$$

and the associated boundary conditions

$$u=0,\ \ or\ \ (N_{xx}+N_{xx}^s)n_x+(N_{xy}+N_{xy}^s)n_y=0 \tag{13a}$$

$$v=0,\ \ or\ \ (N_{xy}+N_{xy}^s)n_x+(N_{yy}+N_{yy}^s)n_y=0 \tag{13b}$$

$$\begin{aligned}&w=0,\ \ or\ \ n_x(\frac{\partial(M_{xx}+M_{xx}^s)}{\partial x}+\frac{\partial(M_{xy}+M_{xy}^s)}{\partial y}+\frac{\partial P_{xxz}}{\partial x}-(N^0+N^T)\frac{\partial w}{\partial x})\\&+n_y(\frac{\partial(M_{yy}+M_{yy}^s)}{\partial y}+\frac{\partial(M_{xy}+M_{xy}^s)}{\partial x}+\frac{\partial P_{yyz}}{\partial y}-(N^0+N^T)\frac{\partial w}{\partial y})=0\end{aligned} \tag{13c}$$

$$\frac{\partial w}{\partial x}=0,\ \ or\ \ (M_{xx}+M_{xx}^s)n_x+(M_{xy}+M_{xy}^s)n_y=0 \tag{13d}$$

$$\frac{\partial w}{\partial y}=0,\ \ or\ \ (M_{xy}+M_{xy}^s)n_x+(M_{yy}+M_{yy}^s)n_y=0 \tag{13e}$$

where $N_x^0=N_y^0=N^T+N^0, N_{xy}^0=0$. For a piezoelectric nanoplate with the flexoelectric effect, the nonlocal constitutive relations for the bulk may be written as

$$\sigma_{xx}-(e_0a)^2\nabla^2\sigma_{xx}=c_{11}\varepsilon_{xx}+c_{12}\varepsilon_{yy}+e_{31}\frac{\partial\varphi}{\partial z}-\frac{f_{31}}{2}\frac{\partial^2\varphi}{\partial z^2}-c_{11}\alpha_1\Delta T \tag{14}$$

$$\sigma_{yy}-(e_0a)^2\nabla^2\sigma_{yy}=c_{12}\varepsilon_{xx}+c_{22}\varepsilon_{yy}+e_{32}\frac{\partial\varphi}{\partial z}-\frac{f_{32}}{2}\frac{\partial^2\varphi}{\partial z^2}-c_{22}\alpha_2\Delta T \tag{15}$$

$$\sigma_{xy}-(e_0a)^2\nabla^2\sigma_{xy}=c_{66}\gamma_{xy} \tag{16}$$

$$\tau_{xxz}-(e_0a)^2\nabla^2\tau_{xxz}=-\frac{f_{31}}{2}\frac{\partial^2\varphi}{\partial z^2} \tag{17}$$

$$\tau_{yyz}-(e_0a)^2\nabla^2\tau_{xxz}=-\frac{f_{32}}{2}\frac{\partial^2\varphi}{\partial z^2} \tag{18}$$

$$D_z-(e_0a)^2\nabla^2 D_z=e_{31}\varepsilon_{xx}+e_{32}\varepsilon_{yy}-k_{33}\frac{\partial\varphi}{\partial z}+\frac{f_{31}}{2}\eta_{xxz}+\frac{f_{32}}{2}\eta_{yyz}+p_3\Delta T \tag{19}$$

$$Q_{zz}-(e_0a)^2\nabla^2 Q_{zz}=-\frac{f_{31}}{2}\varepsilon_{xx}-\frac{f_{32}}{2}\varepsilon_{yy} \tag{20}$$

where φ is the electrostatic potential and $E_z=-\frac{\partial\varphi}{\partial z}$. Also, the nonlocal constitutive relations for the surface layer can be expressed by

$$\sigma_{xx}^s-(e_0a)^2\nabla^2\sigma_{xx}^s=\sigma_{xx}^0+c_{11}^s\varepsilon_{xx}+c_{12}^s\varepsilon_{yy}+e_{31}^s\frac{\partial\varphi}{\partial z} \tag{21}$$

$$\sigma_{yy}^s-(e_0a)^2\nabla^2\sigma_{yy}^s=\sigma_{yy}^0+c_{21}^s\varepsilon_{xx}+c_{22}^s\varepsilon_{yy}+e_{32}^s\frac{\partial\varphi}{\partial z} \tag{22}$$

$$\sigma_{xy}^s-(e_0a)^2\nabla^2\sigma_{xy}^s=c_{66}^s\gamma_{xy} \tag{23}$$

Under the open circuit condition, the electric displacement on the surface is zero. Therefore, one can obtain the electric field an electric field gradient as

$$E_z=-(\frac{e_{31}}{k_{33}}\frac{\partial u}{\partial x}+\frac{e_{32}}{k_{33}}\frac{\partial v}{\partial y})+z(\frac{e_{31}}{k_{33}}\frac{\partial^2 w}{\partial x^2}+\frac{e_{32}}{k_{33}}\frac{\partial^2 w}{\partial y^2})+(\frac{f_{31}}{k_{33}}\frac{\partial^2 w}{\partial x^2}+\frac{f_{32}}{k_{33}}\frac{\partial^2 w}{\partial y^2}) \tag{24}$$

Finally, the electric field gradient can be written as

$$E_{z,z}=\frac{e_{31}}{k_{33}}\frac{\partial^2 w}{\partial x^2}+\frac{e_{32}}{k_{33}}\frac{\partial^2 w}{\partial y^2} \tag{25}$$

Using Eqs. (24) and (25) the nonlocal constitutive relations for the bulk and surface can be expressed by the following form

$$\begin{aligned}&\sigma_{xx}-(e_0a)^2\nabla^2\sigma_{xx}=(c_{11}+\frac{e_{31}^2}{k_{33}})\frac{\partial u}{\partial x}+(c_{12}+\frac{e_{31}e_{32}}{k_{33}})\frac{\partial v}{\partial y}-(c_{11}+\frac{e_{31}^2}{k_{33}})z\frac{\partial^2 w}{\partial x^2}-(c_{12}+\frac{e_{31}e_{32}}{k_{33}})z\frac{\partial^2 w}{\partial y^2}\\&-(\frac{e_{31}f_{31}}{2k_{33}})\frac{\partial^2 w}{\partial x^2}-(\frac{2e_{32}f_{31}-e_{31}f_{32}}{2k_{33}})\frac{\partial^2 w}{\partial y^2}-c_{11}\alpha_1\Delta T\end{aligned} \tag{26}$$

$$\begin{aligned}&\sigma_{yy}-(e_0a)^2\nabla^2\sigma_{yy}=(c_{12}+\frac{e_{32}e_{31}}{k_{33}})\frac{\partial u}{\partial x}+(c_{22}+\frac{e_{32}^2}{k_{33}})\frac{\partial v}{\partial y}-(c_{12}+\frac{e_{32}e_{31}}{k_{33}})z\frac{\partial^2 w}{\partial x^2}-(c_{22}+\frac{e_{32}^2}{k_{33}})z\frac{\partial^2 w}{\partial y^2}\\&-(\frac{2e_{32}f_{31}-e_{31}f_{32}}{2k_{33}})\frac{\partial^2 w}{\partial x^2}-(\frac{e_{32}f_{32}}{2k_{33}})\frac{\partial^2 w}{\partial y^2}-c_{22}\alpha_2\Delta T\end{aligned} \tag{27}$$

$$\sigma_{xy}-(e_0a)^2\nabla^2\sigma_{xy}=c_{66}(\frac{\partial u}{\partial y}+\frac{\partial v}{\partial x}-2z\frac{\partial^2 w}{\partial x\partial y}) \tag{28}$$

$$\begin{aligned}&\tau_{xxz}-(e_0a)^2\nabla^2\tau_{xxz}=(\frac{e_{31}f_{31}}{2k_{33}})\frac{\partial u}{\partial x}+(\frac{e_{32}f_{31}}{2k_{33}})\frac{\partial v}{\partial y}-(\frac{e_{31}f_{31}}{2k_{33}})z\frac{\partial^2 w}{\partial x^2}-(\frac{e_{32}f_{31}}{2k_{33}})z\frac{\partial^2 w}{\partial y^2}\\&-(\frac{f_{31}^2}{k_{33}})\frac{\partial^2 w}{\partial x^2}-(\frac{f_{31}f_{32}}{k_{33}})\frac{\partial^2 w}{\partial y^2}\end{aligned} \tag{29}$$

$$\begin{aligned}&\tau_{yyz}-(e_0a)^2\nabla^2\tau_{xxz}=(\frac{e_{31}f_{32}}{2k_{33}})\frac{\partial u}{\partial x}+(\frac{e_{32}f_{32}}{2k_{33}})\frac{\partial v}{\partial y}-(\frac{e_{31}f_{32}}{2k_{33}})z\frac{\partial^2 w}{\partial x^2}-(\frac{e_{32}f_{32}}{2k_{33}})z\frac{\partial^2 w}{\partial y^2}\\&-(\frac{f_{31}f_{32}}{k_{33}})\frac{\partial^2 w}{\partial x^2}-(\frac{f_{32}^2}{k_{33}})\frac{\partial^2 w}{\partial y^2}\end{aligned} \tag{30}$$

$$\begin{aligned}&\sigma_{xx}^s-(e_0a)^2\nabla^2\sigma_{xx}^s=\sigma_{xx}^0+(c_{11}^s+\frac{e_{31}^se_{31}}{k_{33}})\frac{\partial u}{\partial x}+(c_{12}^s+\frac{e_{31}^se_{32}}{k_{33}})\frac{\partial v}{\partial y}-(c_{11}^s+\frac{e_{31}^se_{31}}{k_{33}})z\frac{\partial^2 w}{\partial x^2}\\&-(c_{12}^s+\frac{e_{31}^se_{32}}{k_{33}})z\frac{\partial^2 w}{\partial y^2}-(\frac{e_{31}^sf_{31}}{k_{33}}\frac{\partial^2 w}{\partial x^2}+\frac{e_{31}^sf_{32}}{k_{33}}\frac{\partial^2 w}{\partial y^2})\end{aligned} \tag{31}$$

$$\begin{aligned}&\sigma_{yy}^s-(e_0a)^2\nabla^2\sigma_{yy}^s=\sigma_{yy}^0+(c_{21}^s+\frac{e_{32}^se_{31}}{k_{33}})\frac{\partial u}{\partial x}+(c_{22}^s+\frac{e_{32}^se_{32}}{k_{33}})\frac{\partial v}{\partial y}-(c_{21}^s+\frac{e_{32}^se_{31}}{k_{33}})z\frac{\partial^2 w}{\partial x^2}\\&-(c_{22}^s+\frac{e_{32}^se_{32}}{k_{33}})z\frac{\partial^2 w}{\partial y^2}-(\frac{e_{32}^sf_{31}}{k_{33}}\frac{\partial^2 w}{\partial x^2}+\frac{e_{32}^sf_{32}}{k_{33}}\frac{\partial^2 w}{\partial y^2})\end{aligned} \tag{32}$$

$$\sigma_{xy}^s-(e_0a)^2\nabla^2\sigma_{xy}^s=c_{66}^s(\frac{\partial u}{\partial y}+\frac{\partial v}{\partial x}-2z\frac{\partial^2 w}{\partial x\partial y}) \tag{33}$$

Therefore, by integrating Eqs. (26)-(30) over the plate's cross-section area, the force and moment stress resultants can be rewritten in the following form

$$N_{xx}-\mu\nabla^2 N_{xx}=A_{11}\frac{\partial u}{\partial x}+A_{12}\frac{\partial v}{\partial y}-B_{11}\frac{\partial^2 w}{\partial x^2}-B_{12}\frac{\partial^2 w}{\partial y^2}-N_{xx}^T \tag{34}$$

$$N_{yy}-\mu\nabla^2 N_{yy}=A_{21}\frac{\partial u}{\partial x}+A_{22}\frac{\partial v}{\partial y}-B_{21}\frac{\partial^2 w}{\partial x^2}-B_{22}\frac{\partial^2 w}{\partial y^2}-N_{yy}^T \tag{35}$$

$$N_{xy}-\mu\nabla^2 N_{xy}=A_{66}(\frac{\partial u}{\partial y}+\frac{\partial v}{\partial x}) \tag{36}$$

$$M_{xx}-\mu\nabla^2 M_{xx}=-C_{11}\frac{\partial^2 w}{\partial x^2}-C_{12}\frac{\partial^2 w}{\partial y^2} \tag{37}$$

$$M_{yy}-\mu\nabla^2 M_{yy}=-C_{21}\frac{\partial^2 w}{\partial x^2}-C_{22}\frac{\partial^2 w}{\partial y^2} \tag{38}$$

$$M_{xy}-\mu\nabla^2 M_{xy}=-C_{66}\frac{\partial^2 w}{\partial x\partial y} \tag{39}$$

$$P_{xxz}-\mu\nabla^2 P_{xxz}=B_{11}\frac{\partial u}{\partial x}+B_{12}\frac{\partial v}{\partial y}-D_{11}\frac{\partial^2 w}{\partial x^2}-D_{12}\frac{\partial^2 w}{\partial y^2} \tag{40}$$

$$P_{yyz}-\mu\nabla^2 P_{yyz}=B_{21}\frac{\partial u}{\partial x}+B_{22}\frac{\partial v}{\partial y}-D_{21}\frac{\partial^2 w}{\partial x^2}-D_{22}\frac{\partial^2 w}{\partial y^2} \tag{41}$$

where $\mu=(e_0a)^2$ and $N_{xx}^T=N_{yy}^T=c_{11}\alpha_1 h\Delta T$. The cross sectional rigidities are defined as

$$\begin{aligned}
&A_{11}=(c_{11}+\frac{e_{31}^2}{k_{33}})bh,\ A_{22}=(c_{22}+\frac{e_{32}^2}{k_{33}})bh,\ A_{12}=A_{21}=(c_{12}+\frac{e_{31}e_{32}}{k_{33}})bh,\ A_{66}=c_{66}bh\\
&B_{11}=(\frac{e_{31}f_{31}}{2k_{33}})bh,\ B_{22}=(\frac{e_{32}f_{32}}{2k_{33}})bh,\ B_{12}=B_{21}=(\frac{2e_{32}f_{31}-e_{31}f_{32}}{2k_{33}})bh,\\
&C_{11}=(c_{11}+\frac{e_{31}^2}{k_{33}})b\frac{h^3}{12},\ C_{22}=(c_{22}+\frac{e_{32}^2}{k_{33}})b\frac{h^3}{12},\ C_{12}=C_{21}=(c_{12}+\frac{e_{31}e_{32}}{k_{33}})b\frac{h^3}{12},\ C_{66}=2c_{66}b\frac{h^3}{12},\\
&D_{11}=(\frac{f_{31}^2}{k_{33}})bh,\ D_{22}=(\frac{f_{32}^2}{k_{33}})bh,\ D_{12}=D_{21}=(\frac{f_{31}f_{32}}{k_{33}})bh
\end{aligned} \tag{42}$$

And the force and moment stress resultants due to surface piezoelasticity may be expressed as

$$N_{xx}^s-\mu\nabla^2 N_{xx}^s=A_{11}^s\frac{\partial u}{\partial x}+A_{12}^s\frac{\partial v}{\partial y}-B_{11}^s\frac{\partial^2 w}{\partial x^2}-B_{12}^s\frac{\partial^2 w}{\partial y^2} \tag{41}$$

$$N_{yy}^s-\mu\nabla^2 N_{yy}^s=A_{21}^s\frac{\partial u}{\partial x}+A_{22}^s\frac{\partial v}{\partial y}-B_{21}^s\frac{\partial^2 w}{\partial x^2}-B_{22}^s\frac{\partial^2 w}{\partial y^2} \tag{42}$$

$$N_{xy}^s-\mu\nabla^2 N_{xy}^s=A_{66}^s(\frac{\partial u}{\partial y}+\frac{\partial v}{\partial x})-A_{66}^{sw}\frac{\partial^2 w}{\partial x\partial y} \tag{43}$$

$$M_{xx}^s-\mu\nabla^2 M_{xx}^s=F_{11}^s\frac{\partial u}{\partial x}+F_{12}^s\frac{\partial v}{\partial y}-C_{11}^s\frac{\partial^2 w}{\partial x^2}-C_{12}^s\frac{\partial^2 w}{\partial y^2} \tag{44}$$

$$M_{yy}^s-\mu\nabla^2 M_{yy}^s=F_{21}^s\frac{\partial u}{\partial x}+F_{22}^s\frac{\partial v}{\partial y}-C_{21}^s\frac{\partial^2 w}{\partial x^2}-C_{22}^s\frac{\partial^2 w}{\partial y^2} \tag{45}$$

$$M_{xy}^s-\mu\nabla^2 M_{xy}^s=C_{66}^{sw}(\frac{\partial u}{\partial y}+\frac{\partial v}{\partial x})-C_{66}^s\frac{\partial^2 w}{\partial x\partial y} \tag{46}$$

in which

$$\begin{aligned}
&A_{11}^s=2(c_{11}^s+\frac{e_{31}e_{31}^s}{k_{33}})h,\quad A_{22}^s=2(c_{22}^s+\frac{e_{32}e_{32}^s}{k_{33}})h,\quad A_{12}^s=A_{21}^s=2(c_{12}^s+\frac{e_{32}e_{31}^s}{k_{33}})h,\\
&A_{66}^s=2c_{66}^s h,\quad A_{66}^{sw}=c_{66}^s bh^2,\quad B_{11}^s=(c_{11}^s+\frac{e_{31}e_{31}^s}{k_{33}})\frac{bh^2}{2}+2(\frac{e_{31}^s f_{31}}{k_{33}})h,\\
&B_{22}^s=(c_{22}^s+\frac{e_{32}e_{32}^s}{k_{33}})\frac{bh^2}{2}+2(\frac{e_{32}^s f_{32}}{k_{33}})h,\quad B_{12}^s=B_{21}^s=(c_{12}^s+\frac{e_{32}e_{31}^s}{k_{33}})\frac{bh^2}{2}+2(\frac{e_{31}^s f_{32}}{k_{33}})h,\\
&F_{11}^s=(c_{11}^s+\frac{e_{31}e_{31}^s}{k_{33}})\frac{bh^2}{2},\quad F_{22}^s=(c_{22}^s+\frac{e_{32}e_{32}^s}{k_{33}})\frac{bh^2}{2},\quad F_{12}^s=F_{21}^s=(c_{12}^s+\frac{e_{32}e_{31}^s}{k_{33}})\frac{bh^2}{2},\\
&C_{11}^s=(c_{11}^s+\frac{e_{31}e_{31}^s}{k_{33}})\frac{h^3}{6}+(\frac{e_{31}^s f_{31}}{k_{33}})\frac{bh^2}{2},\quad C_{22}^s=(c_{22}^s+\frac{e_{32}e_{32}^s}{k_{33}})\frac{h^3}{6}+(\frac{e_{32}^s f_{32}}{k_{33}})\frac{bh^2}{2},\\
&C_{12}^s=(c_{12}^s+\frac{e_{32}e_{31}^s}{k_{33}})\frac{h^3}{6}+(\frac{e_{31}^s f_{32}}{k_{33}})\frac{bh^2}{2},\ C_{66}^s=c_{66}^s\frac{h^3}{3},C_{66}^{sw}=c_{66}^s\frac{bh^2}{2}.
\end{aligned} \tag{49}$$

The nonlocal governing equations of a piezoelectric nanoplate with surface and flexoelectric effects in terms of the displacement can be derived by substituting Eqs. (34)-(48), into Eq. (12) as follows

$$\begin{aligned}
&(A_{11}+A_{11}^s)\frac{\partial^2 u}{\partial x^2}+(A_{66}+A_{66}^s)\frac{\partial^2 u}{\partial y^2}+(A_{12}+A_{12}^s+A_{66}+A_{66}^s)\frac{\partial^2 v}{\partial x\partial y}-(B_{11}+B_{11}^s)\frac{\partial^3 w_b}{\partial x^3}\\
&-(B_{12}+B_{12}^s)\frac{\partial^3 w}{\partial x\partial y^2}-A_{66}^{sw}\frac{\partial^2 w}{\partial x\partial y^2}=0
\end{aligned} \tag{50}$$

$$\begin{aligned}
&(A_{66}+A_{66}^s)\frac{\partial^2 v}{\partial x^2}+(A_{22}+A_{22}^s)\frac{\partial^2 v}{\partial y^2}+(A_{21}+A_{21}^s+A_{66}+A_{66}^s)\frac{\partial^2 u}{\partial x\partial y}-(B_{22}+B_{22}^s)\frac{\partial^3 w}{\partial y^3}\\
&-(B_{21}+B_{21}^s)\frac{\partial^3 w}{\partial x^2\partial y}-A_{66}^{sw}\frac{\partial^3 w}{\partial x^2\partial y}=0
\end{aligned} \tag{51}$$

$$\begin{aligned}
&(B_{11}+F_{11}^s)\frac{\partial^3 u}{\partial x^3}+(B_{12}+F_{12}^s+2C_{66}^{sw})\frac{\partial^3 u}{\partial x\partial y^2}+(B_{12}+F_{21}^s+2C_{66}^{sw})\frac{\partial^3 v}{\partial x^2\partial y}+(B_{22}+F_{22}^s)\frac{\partial^3 v}{\partial y^3}\\
&-(C_{11}+C_{11}^s+D_{11})\frac{\partial^4 w}{\partial x^4}-2(C_{12}+C_{12}^s+C_{66}+C_{66}^s+D_{12})\frac{\partial^4 w}{\partial x^4\partial y^2}-(C_{22}+C_{22}^s+D_{22})\frac{\partial^4 w}{\partial y^4}\\
&-b(N^T+N^0)(\frac{\partial^2 w}{\partial x^2}+\frac{\partial^2 w}{\partial y^2})+2b\sigma_0(\frac{\partial^2 w}{\partial x^2}+\frac{\partial^2 w}{\partial y^2})+\mu b(N^T+N^0)(\frac{\partial^2}{\partial x^2}+\frac{\partial^2}{\partial y^2})(\frac{\partial^2 w}{\partial x^2}+\frac{\partial^2 w}{\partial y^2})\\
&-\mu 2b\sigma_0(\frac{\partial^2}{\partial x^2}+\frac{\partial^2}{\partial y^2})(\frac{\partial^2 w}{\partial x^2}+\frac{\partial^2 w}{\partial y^2})=0
\end{aligned} \tag{52}$$

4. Solution procedure

In this section, an analytical solution of the governing equations for thermal bucking of a flexoelectric nanoplate with simply-supported (*S*), clamped (*C*) or free (*F*) edges or combinations of these boundary conditions is presented which they are given as:

- Simply-supported (S)

$$\begin{aligned}
&v=w=N_{xx}=M_{xx}=0 \qquad \text{at x=0,a}\\
&u=w=N_{yy}=M_{yy}=0 \qquad \text{at y=0,b}
\end{aligned} \tag{53}$$

- Clamped (C)

$$u=v=w=0 \qquad \text{at x=0,a and y=0,b} \tag{54}$$

To satisfy above-mentioned boundary conditions, the displacement quantities are presented in the following form

$$u=\sum_{m=1}^{\infty}\sum_{n=1}^{\infty}U_{mn}\frac{\partial X_m(x)}{\partial x}Y_n(y) \tag{55}$$

$$v=\sum_{m=1}^{\infty}\sum_{n=1}^{\infty}V_{mn}X_m(x)\frac{\partial Y_n(y)}{\partial y} \tag{56}$$

$$w=\sum_{m=1}^{\infty}\sum_{n=1}^{\infty}W_{mn}X_m(x)Y_n(y) \tag{57}$$

where (U_{mn}, V_{mn}, W_{mn}) are the unknown coefficients. Inserting Eqs. (55)-(57) into Eqs. (50)-(52) respectively, leads to

$$\left\{\begin{pmatrix} k_{1,1} & k_{1,2} & k_{1,3} \\ k_{2,1} & k_{2,2} & k_{2,3} \\ k_{3,1} & k_{3,2} & k_{3,3} \end{pmatrix}\right\}\begin{Bmatrix} U_{mn} \\ V_{mn} \\ W_{mn} \end{Bmatrix}=0 \tag{58}$$

where

$$k_{1,1}=(A_{11}+A_{11}^{s})\kappa_{12}+(A_{66}+A_{66}^{s})\kappa_{8},\quad k_{1,2}=\left(A_{12}+A_{12}^{s}+A_{66}+A_{66}^{s}\right)\kappa_{10},$$
$$k_{1,3}=(B_{11}+F_{11}^{s})\kappa_{13}+\left(B_{12}+F_{12}^{s}-2C_{66}^{sw}\right)\kappa_{11},$$
$$k_{2,1}=\left(A_{12}+A_{12}^{s}+A_{66}+A_{66}^{s}\right)\kappa_{8},$$
$$k_{2,2}=(A_{22}+A_{22}^{s})\kappa_{4}+(A_{66}+A_{66}^{s})\kappa_{10},$$
$$k_{2,3}=(B_{22}+F_{22}^{s})\kappa_{5}+(B_{12}+F_{12}^{s}-2C_{66}^{sw})\kappa_{11},$$
$$k_{3,1}=(B_{11}+F_{11}^{s})\kappa_{12}+\left(B_{12}+F_{12}^{s}-2C_{66}^{s}\right)\kappa_{8},$$
$$k_{3,3}=-(C_{11}+C_{11}^{s}+D_{11})\kappa_{13}-2\left(C_{12}+C_{12}^{s}+C_{66}+C_{66}^{s}+D_{12}\right)\kappa_{11}-(C_{22}+C_{22}^{s}+D_{22})\kappa_{13}\kappa_{5}$$
$$-b(N^{T}+N^{0}+2\sigma_{0})\left(\kappa_{3}+\kappa_{9}\right)+\mu b(N^{T}+N^{0}+2\sigma_{0})\left(\kappa_{5}+\kappa_{13}+2\kappa_{11}\right)$$

in which

$$(\kappa_1,\kappa_3,\kappa_5)=\int_0^a\int_0^b(X_mY_n,\ X_mY_n'',\ X_mY_n'''')X_mY_n\,dxdy$$
$$(\kappa_9,\kappa_{11},\kappa_{13})=\int_0^a\int_0^b(X_m''Y_n,\ X_m''Y_n'',\ X_m''''Y_n)X_mY_n\,dxdy$$
$$(\kappa_6,\kappa_8,\kappa_{12})=\int_0^a\int_0^b(X_m'Y_n,\ X_m'Y_n'',\ X_m'''Y_n)X_m'Y_n\,dxdy$$
$$(\kappa_2,\kappa_4,\kappa_{10})=\int_0^a\int_0^b(X_mY_n',\ X_mY_n''',\ X_m''Y_n')X_mY_n'\,dxdy$$

By finding determinant of the coefficients of above matrix and setting it to zero, we can find critical buckling temperatures. The function X_m for different boundary conditions is defined by

SS:
$$X_m(x)=\sin(\lambda_m x)$$
$$\lambda_m=\frac{n\pi}{a} \tag{59}$$

CC:
$$X_m(x)=\sin(\lambda_m x)-\sinh(\lambda_m x)-\xi_m(\cos(\lambda_m x)-\cosh(\lambda_m x))$$
$$\xi_m=\frac{\sin(\lambda_m x)-\sinh(\lambda_m x)}{\cos(\lambda_m x)-\cosh(\lambda_m x)} \tag{60}$$
$$\lambda_1=4.730,\lambda_2=7.853,\lambda_3=10.996,\lambda_4=14.137,\quad \lambda_{m\geq 5}=\frac{(m+0.5)\pi}{a}$$

CS:
$$X_m(x)=\sin(\lambda_m x)-\sinh(\lambda_m x)-\xi_m(\cos(\lambda_m x)-\cosh(\lambda_m x))$$
$$\xi_m=\frac{\sin(\lambda_m x)+\sinh(\lambda_m x)}{\cos(\lambda_m x)+\cosh(\lambda_m x)} \tag{61}$$
$$\lambda_1=3.927,\lambda_2=7.069,\lambda_3=10.210,\lambda_4=13.352,\quad \lambda_{m\geq 5}=\frac{(m+0.25)\pi}{a}$$

The function Y_n can be obtained by replacing x, m and a, respectively by y, n and b.

5. Types of thermal loadings

Temperature rise in structure may led to thermal buckling phenomena. Different temperature distributions can be find in the literature:

5.1 Uniform temperature rise

Assume the case that the temperature of the nanoplate uniformly raised through-the-thickness as

$$T(z)=\Delta T. \tag{62}$$

Therefore, the pre-buckling force N^T is

$$N^{T}=c_{11}\alpha_1 h\Delta T \tag{63}$$

5.2 Linear temperature rise

Now let us consider the temperature rise varies linearly across the nanoplate thickness as

$$T(z)=T_0+\Delta T(\frac{z}{h}+\frac{1}{2}) \tag{64}$$

The pre-buckling force N^T is

$$N^{T}=\frac{1}{2}c_{11}\alpha_1 h\Delta T \tag{65}$$

Also, for better presentation of the results the following dimensionless quantity is adopted

$$\bar{N}=\mathrm{N}^0\frac{\mathrm{a}^2}{D},\quad D=c_{11}h^3 \tag{66}$$

6. Numerical results and discussions

Thermal buckling of nonlocal flexoelectric nanoplates under uniform and linear temperature rise incorporating surface effect is examined. It is considered that the flexoelectric nanoplate is made of PZT-5H where the elastic

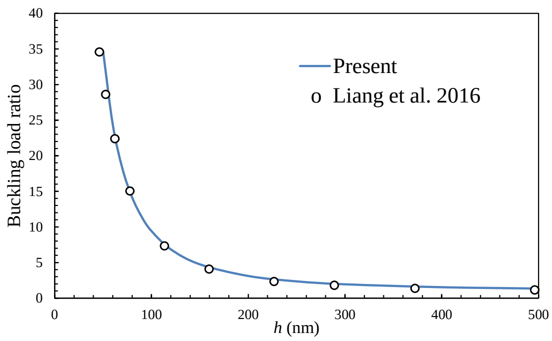

Fig. 2 Comparison of buckling load ratio of flexoelectric nanoplates without surface and nonlocal effects

properties are considered as c_{11}=102 Gpa, c_{12}=31 Gpa, c_{66}=35.5 Gpa and the piezoelectric and dielectric coefficients are assumed as e_{31}=17.05 C/m^2 and k_{33}=1.76×10^{-8} C/(Vm). The flexoelectric coefficient is also considered as f_{31}=10^{-7} (Yang *et al.* 2015). The surface elastic and piezoelectric constants for PZT-5H can be considered as: c_{11}^s =102 N/m, c_{12}^s =31 N/m, c_{66}^s =35.5 N/m and e_{31}^s =11 C/m. Comparison is performed with those of a flexoelectric nanoplate presented by Liang *et al.* (2016). To this end, effect of nonlocality, surface elasticity, surface piezoelasticity and elastic foundation are omitted. In Fig. 2 the buckling load ratio ($N^{0\ \text{with flexoelectric}}/N^{0\ \text{without flexoelectric}}$) is presented as a function of nanoplate thickness. The results are in an excellent agreement with those of Liang *et al.* (2016) for a simply-supported flexoelectric nanoplate.

Fig. 3 shows the variation of buckling load of NL and NL-SE piezoelectric nanoplates under uniform temperature change versus thickness (h) with and without flexoelectric effect when a=1000 nm, ΔT=50. In this figure, SSSS and CCCC flexoelectric nanoplates are assumed. It is concluded that neglecting the surface effect leads to lower buckling loads. In fact, inclusion of surface effect enhances the stiffness of flexoelectric nanoplates and buckling loads increases. Also, buckling loads reduce with increase of nanoplate thickness. But, this reduction in buckling loads with respect to thickness depends on the flexoelectricity effect. It means that effect of flexoelectricity becomes less important at large thicknesses. In fact, at smaller thicknesses the strain gradients increase and the effect of flexoelectricity becomes more prominent. So, flexoelectricity presents an inherent size effect and can be neglected in analysis of large scale plates. It can be deduced that the buckling loads predicted by the nonlocal flexoelectric plate model are consistently larger than those of the conventional nonlocal plate model without considering flexoelectricity.

Effect of flexoelectricity on buckling load of piezoelectric nanoplates under uniform and linear temperature changes at a=1000 nm and ΔT=300 is presented in Fig. 4. As previously mentioned, neglecting flexoelectricity effects leads to lower buckling loads for all values of nanoplate thickness. Also, for all values of nanoplate's thickness, the magnitude of buckling load

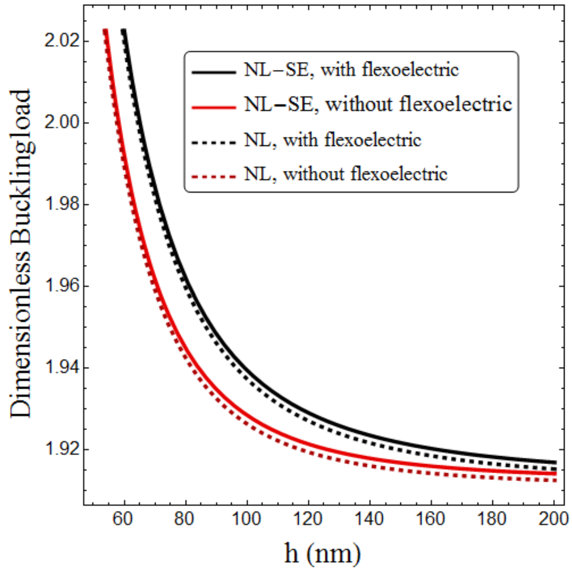

(a) SSSS

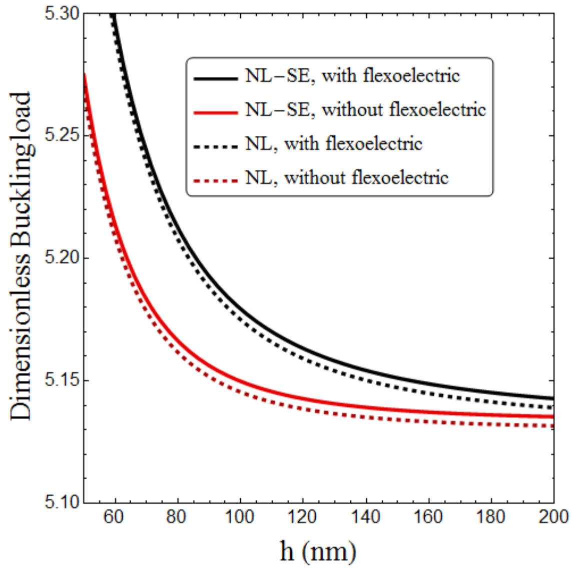

(b) CCCC

Fig. 3 Variation of buckling load of NL and NL-SE piezoelectric nanoplates under uniform temperature change with and without flexoelectric effect (a=1000 nm, ΔT=50)

depends on the type of thermal loading. It is known that nanoplate under uniform temperature rise (UTR) is more flexible than linear temperature rise (LTR). So, LTR gives larger buckling loads for a piezoelectric nanoplate with and without flexoelectric effect. Such observations are valid for both SSSS and CCCC nanoplates.

Effect of temperature change (ΔT) on buckling load of flexoelectric nanoplates under uniform temperature change with respect to thickness of plate is plotted in Fig. 5 for SSSS and CCCC boundary conditions. It is seen that as the value of thickness increase, buckling load significantly reduces. But, larger values of thickness have no sensible effect on dimensionless buckling loads of flexoelectric nanoplate. Also, it should be stated that effect of temperature change is neglected in all previous papers on flexoelectric nanoplates. It is seen that temperature change

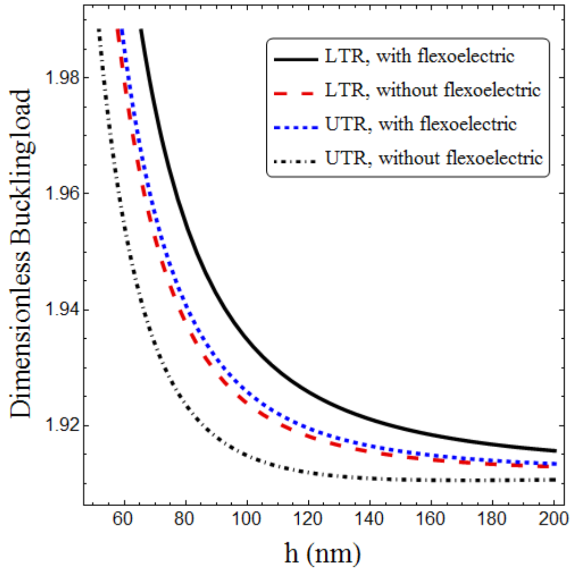

(a) SSSS

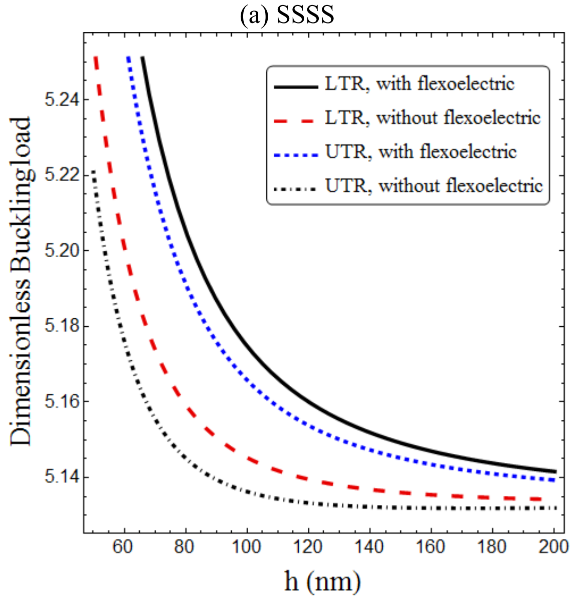

(b) CCCC

Fig. 4 Effect of flexoelectricity on buckling load of piezoelectric nanoplates under uniform and linear temperature changes (a=1000 nm, ΔT=300)

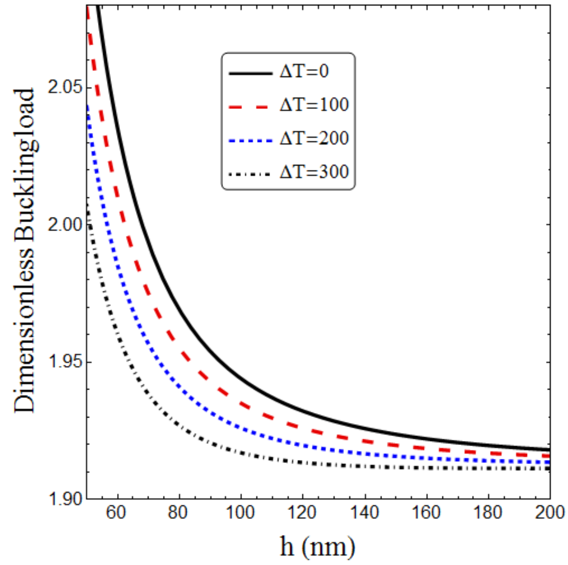

(a) SSSS

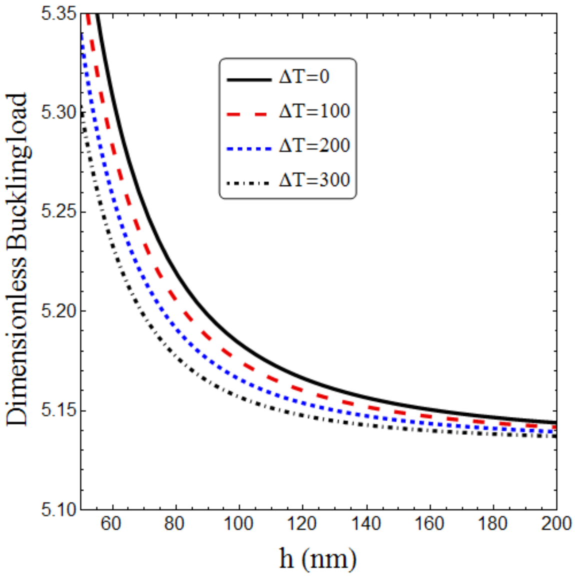

(b) CCCC

Fig. 5 Effect of temperature change on buckling load of flexoelectric nanoplates under uniform temperature change (a=1000 nm)

significantly affects the buckling loads of flexoelectric nanoplates for every value of thickness.

In fact, increase of temperature reduces the stiffness of flexoelectric nanoplate and leads to lower buckling loads. But, effect of temperature change is more prominent at lower thicknesses. In other words, thinner flexoelectric nanoplates are more affected by the temperature rise.

Fig. 6 illustrates the influence of nonlocal parameter and temperature change on buckling load of flexoelectric nanoplates under uniform temperature change with surface effects at a=100 nm, h=10 nm. It is observable that a nonlocal flexoelectric nanoplate has lower critical buckling loads compared with local flexoelectric nanoplate (μ=0 nm^2), regardless of the type of boundary conditions. So, inclusion of nonlocal stress field parameter reduces the buckling loads of a flexoelectric nanoplate. In fact, nonlocal parameter introduces a stiffness-softening impact. So, by neglecting the nonlocal parameter, buckling loads of flexoelectric nanoplate are overestimated. Also, it is clear that buckling behavior of flexoelectric nanoplates relies on the temperature change for every value of nonlocal parameter. At a fixed nonlocal parameter, a rise in temperature leads to lower buckling loads.

Effects of thermal loading and plate aspect ratio (a/b) on buckling load of flexoelectric nanoplates under uniform and linear temperature changes with surface effect are depicted in Fig. 7 at a=1000 nm, h=10 nm, μ=2 nm^2. Regardless of the type of thermal loading, buckling load of flexoelectric nanoplate increases with the rise of plate aspect ratio. Also, it is found that effect of aspect ratio on CCCC flexoelectric nanoplates is more prominent than SSSS one. All these observations are dependent on the type of thermal loading

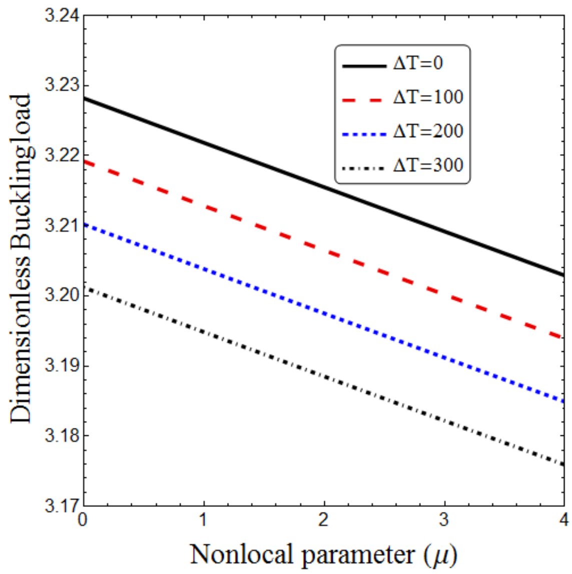

(a) SSSS

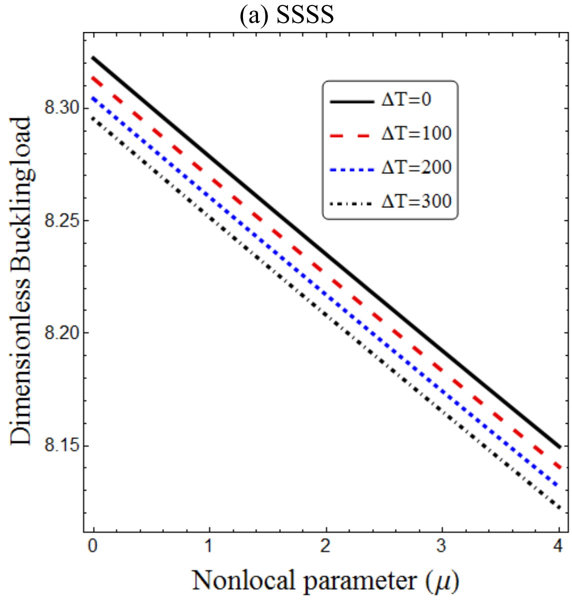

(b) CCCC

Fig. 6 Effect of nonlocal parameter and temperature change on buckling load of flexoelectric nanoplates under uniform temperature change with surface effect (a=100 nm, h=10 nm)

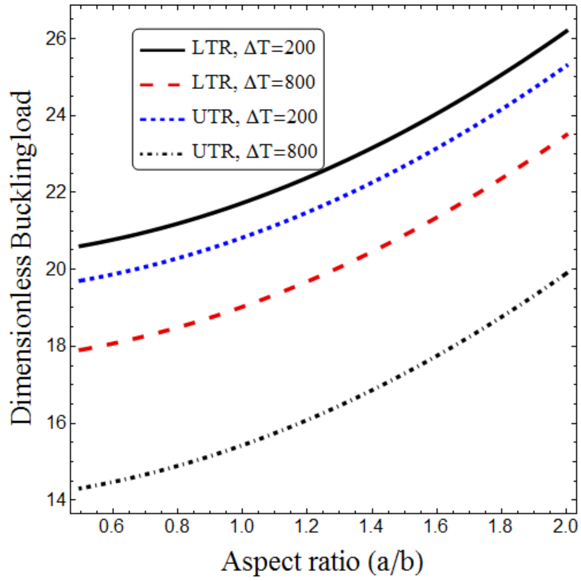

(a) SSSS

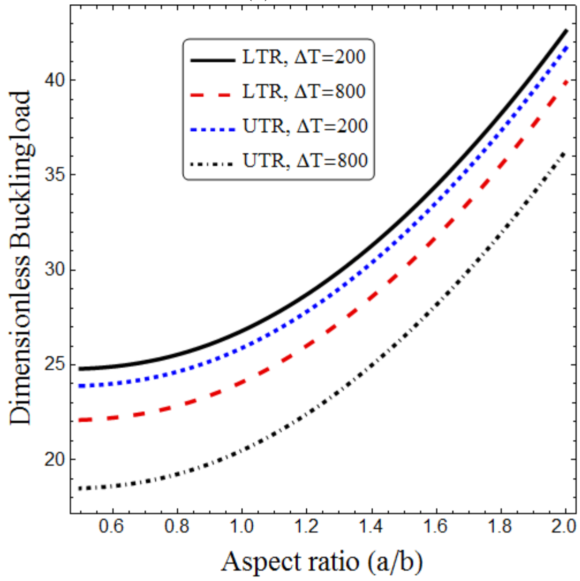

(b) CCCC

Fig. 7 Effect of thermal loading and plate aspect ratio on buckling load of flexoelectric nanoplates under uniform and linear temperature changes with surface effect (a=1000 nm, h=10 nm, μ=2 nm^2)

and also, temperature change value. In other words, increase of temperature shows a reducing impact on buckling loads for every value of aspect ratio. Moreover, for both CCCC and SSSS flexoelectric nanoplates, LTR gives larger buckling loads than UTR at a fixed temperature change and plate aspect ratio.

Another investigation on the effect of aspect ratio on buckling loads of flexoelectric nanoplates under various boundary conditions (SSSS, CSSS, CSCS and CCCC) is illustrated in Fig. 8. It is assumed in this figure that h=10 nm and μ=2 nm^2. As previously mentioned, increase of plate aspect ratio leads to higher buckling loads. But, this increment in buckling load due to aspect ratio depends on the type of boundary condition. By increasing the number of clamped edges, the flexoelectric becomes more rigid and buckling loads will rise. Although, buckling loads of CSSS and CSCS flexoelectric nanoplates are close at lower aspect ratios. But, the difference in buckling loads of CSSS and CSCS nanoplate becomes more significant at larger aspect ratios.

7. Conclusions

In this research, critical buckling characteristics of a flexoelectric nanoplate under uniform and linear thermal loadings are investigated based on nonlocal elasticity theory considering surface effects. This non-classical nanoplate model contains flexoelectric effect to capture coupling of strain gradients and electrical polarizations. Moreover, the

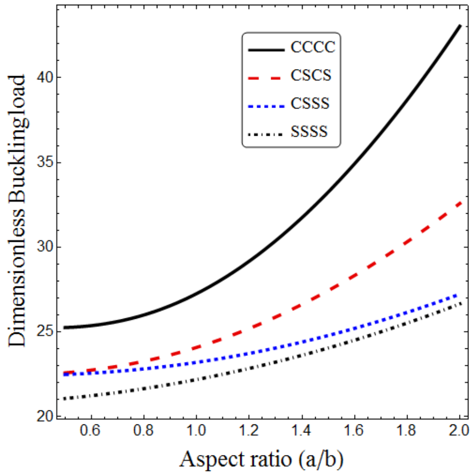

Fig. 8 Effect of boundary condition and plate aspect ratio on buckling load of flexoelectric nanoplates under linear temperature change with surface effect (a=1000 nm, h=10 nm, μ=2 nm^2)

nonlocal elasticity theory is employed to study the nonlocal and long-range interactions between the particles. The present model can degenerate into the classical model if the nonlocal parameter, flexoelectric and surface effects are omitted. Hamilton's principle is employed to derive the governing equations and the related boundary conditions which are solved applying a Galerkin-based solution. From the results analyzed above, it is found that inclusion of nonlocal parameter leads to lower buckling loads by reducing the bending stiffness of NL-SE flexoelectric nanoplates, while ignoring the surface effect leads to reduction in buckling loads. Besides, the non-dimensional buckling loads are found to be decreased by increasing the thickness value, however effect of flexoelectricity on buckling loads is more prominent at lower thicknesses. Increase of temperature reduces the stiffness of flexoelectric nanoplate and leads to lower buckling loads. But, effect of temperature change is more prominent at lower thicknesses. However, a flexoelectric under linear temperature rise has larger buckling loads compared with a flexoelectric nanoplate under uniform temperature rise.

References

Ansari, R., Oskouie, M.F., Gholami, R. and Sadeghi, F. (2016), "Thermo-electro-mechanical vibration of postbuckled piezoelectric Timoshenko nanobeams based on the nonlocal elasticity theory", *Compos. Part B: Eng.*, **89**, 316-327.

Asemi, H.R., Asemi, S.R., Farajpour, A. and Mohammadi, M. (2015), "Nanoscale mass detection based on vibrating piezoelectric ultrathin films under thermo-electro-mechanical loads", *Phys. E: Low-Dimens. Syst. Nanostruct.*, **68**, 112-122.

Asemi, S.R., Farajpour, A., Asemi, H.R. and Mohammadi, M. (2014), "Influence of initial stress on the vibration of double-piezoelectric-nanoplate systems with various boundary conditions using DQM", *Phys. E: Low-Dimens. Syst. Nanostruct.*, **63**, 169-179.

Ebrahimi, F. and Barati, M.R. (2016a), "A nonlocal higher-order shear deformation beam theory for vibration analysis of size-dependent functionally graded nanobeams", *Arab. J. Sci. Eng.*, **41**(5), 1679-1690.

Ebrahimi, F. and Barati, M.R. (2016b), "Small scale effects on hygro-thermo-mechanical vibration of temperature dependent nonhomogeneous nanoscale beams", *Mech. Adv. Mater. Struct.*, Just Accepted.

Ebrahimi, F. and Barati, M.R. (2016c), "Size-dependent thermal stability analysis of graded piezomagnetic nanoplates on elastic medium subjected to various thermal environments", *Appl. Phys. A*, **122**(10), 910.

Ebrahimi, F. and Barati, M.R. (2016d), "Static stability analysis of smart magneto-electro-elastic heterogeneous nanoplates embedded in an elastic medium based on a four-variable refined plate theory", *Smart Mater. Struct.*, **25**(10), 105014.

Ebrahimi, F. and Barati, M.R. (2016e), "Buckling analysis of piezoelectrically actuated smart nanoscale plates subjected to magnetic field", *J. Intell. Mater. Syst. Struct.*, **28**(11), 1472-1490.

Ebrahimi, F. and Barati, M.R. (2016f), "A nonlocal higher-order shear deformation beam theory for vibration analysis of size-dependent functionally graded nanobeams", *Arab. J. Sci. Eng.*, **41**(5), 1679-1690.

Ebrahimi, F. and Barati, M.R. (2016g), "Vibration analysis of nonlocal beams made of functionally graded material in thermal environment", *Eur. Phys. J. Plus*, **131**(8), 279.

Ebrahimi, F. and Barati, M.R. (2016h), "Dynamic modeling of a thermo-piezo-electrically actuated nanosize beam subjected to a magnetic field", *Appl. Phys. A*, **122**(4), 1-18.

Ebrahimi, F. and Barati, M.R. (2016i), "A unified formulation for dynamic analysis of nonlocal heterogeneous nanobeams in hygro-thermal environment", *Appl. Phys. A*, **122**(9), 792.

Ebrahimi, F. and Barati, M.R. (2016j), "A nonlocal higher-order refined magneto-electro-viscoelastic beam model for dynamic analysis of smart nanostructures", *Int. J. Eng. Sci.*, **107**, 183-196.

Ebrahimi, F. and Barati, M.R. (2016k), "Hygrothermal effects on vibration characteristics of viscoelastic FG nanobeams based on nonlocal strain gradient theory", *Compos. Struct.*, **159**, 433-444.

Ebrahimi, F. and Barati, M.R. (2016l), "Buckling analysis of nonlocal third-order shear deformable functionally graded piezoelectric nanobeams embedded in elastic medium", *J. Brazil. Soc. Mech. Sci. Eng.*, **39**(3), 937-952.

Ebrahimi, F. and Barati, M.R. (2016m), "Magnetic field effects on buckling behavior of smart size-dependent graded nanoscale beams", *Eur. Phys. J. Plus*, **131**(7), 1-14.

Ebrahimi, F. and Barati, M.R. (2016n), "Buckling analysis of smart size-dependent higher order magneto-electro-thermo-elastic functionally graded nanosize beams", *J. Mech.*, **33**(1), 23-33.

Ebrahimi, F. and Barati, M.R. (2016o), "An exact solution for buckling analysis of embedded piezoelectro-magnetically actuated nanoscale beams", *Adv. Nano Res.*, **4**(2), 65-84.

Ebrahimi, F. and Barati, M.R. (2016p), "Electromechanical buckling behavior of smart piezoelectrically actuated higher-order size-dependent graded nanoscale beams in thermal environment", *Int. J. Smart Nano Mater.*, **7**(2), 69-90.

Ebrahimi, F. and Barati, M.R. (2016q), "Small scale effects on hygro-thermo-mechanical vibration of temperature dependent nonhomogeneous nanoscale beams", *Mech. Adv. Mater. Struct.*, Just Accepted.

Ebrahimi, F. and Barati, M.R. (2017), "A nonlocal strain gradient refined beam model for buckling analysis of size-dependent shear-deformable curved FG nanobeams", *Compos. Struct.*, **159**, 174-182.

Ebrahimi, F. and Boreiry, M. (2015), "Investigating various surface effects on nonlocal vibrational behavior of nanobeams", *Appl. Phys. A*, **121**(3), 1305-1316.

Ebrahimi, F. and Dabbagh, A. (2016), "On flexural wave

propagation responses of smart FG magneto-electro-elastic nanoplates via nonlocal strain gradient theory", *Compos. Struct.*, **162**, 281-293.
Ebrahimi, F. and Hosseini, S.H.S. (2016a), "Thermal effects on nonlinear vibration behavior of viscoelastic nanosize plates", *J. Therm. Stress.*, **39**(5), 606-625.
Ebrahimi, F. and Hosseini, S.H.S. (2016b), "Double nanoplate-based NEMS under hydrostatic and electrostatic actuations", *Eur. Phys. J. Plus*, **131**(5), 1-19.
Ebrahimi, F. and Salari, E (2015c), "Nonlocal thermo-mechanical vibration analysis of functionally graded nanobeams in thermal environment", *Acta Astronaut.*, **113**, 29-50.
Ebrahimi, F. and Salari, E. (2015a), "Thermal buckling and free vibration analysis of size dependent Timoshenko FG nanobeams in thermal environments", *Compos. Struct.*, **128**, 363-380.
Ebrahimi, F. and Salari, E. (2015b), "Size-dependent free flexural vibrational behavior of functionally graded nanobeams using semi-analytical differential transform method", *Compos. Part B: Eng.*, **79**, 156-169.
Ebrahimi, F., Barati, M.R. and Dabbagh, A. (2016), "A nonlocal strain gradient theory for wave propagation analysis in temperature-dependent inhomogeneous nanoplates", *Int. J. Eng. Sci.*, **107**, 169-182.
Ebrahimi, F., Ghadiri, M., Salari, E., Hoseini, S.A.H. and Shaghaghi, G.R. (2015a), "Application of the differential transformation method for nonlocal vibration analysis of functionally graded nanobeams", *J. Mech. Sci. Technol.*, **29**(3), 1207-1215.
Ebrahimi, F., Salari, E. and Hosseini, S.A.H. (2016), "In-plane thermal loading effects on vibrational characteristics of functionally graded nanobeams", *Meccan.*, **51**(4), 951-977.
Ebrahimi, F., Salari, E., Hosseini, S.A.H. (2015b), "Thermomechanical vibration behavior of FG nanobeams subjected to linear and nonlinear temperature distributions", *J. Therm. Stress.*, **38**(12), 1360-1386.
Ebrahimi, F., Shaghaghi, G.R. and Boreiry, M. (2016), "An investigation into the influence of thermal loading and surface effects on mechanical characteristics of nanotubes", *Struct. Eng. Mech.*, **57**(1), 179-200.
Eringen, A.C. (1972), "Nonlocal polar elastic continua", *Int. J. Eng. Sci.*, **10**(1), 1-16.
Eringen, A.C. (1983), "On differential equations of nonlocal elasticity and solutions of screw dislocation and surface waves", *J. Appl. Phys.*, **54**(9), 4703-4710.
Gurtin, M.E. and Murdoch, A.I. (1975), "A continuum theory of elastic material surfaces", *Arch. Rat. Mech. Analy.*, **57**(4), 291-323.
Hosseini, M., Jamalpoor, A. and Fath, A. (2016), "Surface effect on the biaxial buckling and free vibration of FGM nanoplate embedded in visco-Pasternak standard linear solid-type of foundation", *Meccan.*, **52**(6), 1381-1396.
Jiang, X., Huang, W. and Zhang, S. (2013), "Flexoelectric nano-generator: Materials, structures and devices", *Nano Energy*, **2**(6), 1079-1092.
Ke, L.L. and Wang, Y.S. (2012), "Thermoelectric-mechanical vibration of piezoelectric nanobeams based on the nonlocal theory", *Smart Mater. Struct.*, **21**(2), 025018.
Li, L., Li, X. and Hu, Y. (2016), "Free vibration analysis of nonlocal strain gradient beams made of functionally graded material", *Int. J. Eng. Sci.*, **102**, 77-92.
Li, Y.S. and Pan, E. (2016), "Bending of a sinusoidal piezoelectric nanoplate with surface effect", *Compos. Struct.*, **136**, 45-55.
Liang, X., Hu, S. and Shen, S. (2014), "Effects of surface and flexoelectricity on a piezoelectric nanobeam", *Smart Mater. Struct.*, **23**(3), 035020.
Liang, X., Hu, S. and Shen, S. (2015), "Size-dependent buckling and vibration behaviors of piezoelectric nanostructures due to flexoelectricity", *Smart Mater. Struct.*, **24**(10), 105012.
Liang, X., Yang, W., Hu, S. and Shen, S. (2016), "Buckling and vibration of flexoelectric nanofilms subjected to mechanical loads", *J. Phys. D: Appl. Phys.*, **49**(11), 115307.
Liu, C., Ke, L.L., Wang, Y.S. and Yang, J. (2015), "Nonlinear vibration of nonlocal piezoelectric nanoplates", *Int. J. Struct. Stab. Dyn.*, **15**(8), 1540013.
Liu, C., Ke, L.L., Wang, Y.S., Yang, J. and Kitipornchai, S. (2013), "Thermo-electro-mechanical vibration of piezoelectric nanoplates based on the nonlocal theory", *Compos. Struct.*, **106**, 167-174.
Liu, C., Ke, L.L., Wang, Y.S., Yang, J. and Kitipornchai, S. (2014), "Buckling and post-buckling of size-dependent piezoelectric Timoshenko nanobeams subject to thermo-electro-mechanical loadings", *Int. J. Struct. Stab. Dyn.*, **14**(3), 1350067.
Liu, C., Ke, L.L., Yang, J., Kitipornchai, S. and Wang, Y.S. (2016), "Nonlinear vibration of piezoelectric nanoplates using nonlocal Mindlin plate theory", *Mech. Adv. Mater. Struct.*, Just Accepted.
Ochs, S., Li, S., Adams, C. and Melz, T. (2017), *Efficient Experimental Validation of Stochastic Sensitivity Analyses of Smart Systems*, Smart Structures and Materials, Springer International Publishing.
Salehipour, H., Shahidi, A.R. and Nahvi, H. (2015), "Modified nonlocal elasticity theory for functionally graded materials", *Int. J. Eng. Sci.*, **90**, 44-57.
Wang, K.F. and Wang, B.L. (2011), "Vibration of nanoscale plates with surface energy via nonlocal elasticity", *Phys. E: Low-Dimens. Syst. Nanostruct.*, **44**(2), 448-453.
Wang, K.F. and Wang, B.L. (2012), "The electromechanical coupling behavior of piezoelectric nanowires: Surface and small-scale effects", *Europhys. Lett.*, **97**(6), 66005.
Wang, W., Li, P., Jin, F. and Wang, J. (2016), "Vibration analysis of piezoelectric ceramic circular nanoplates considering surface and nonlocal effects", *Compos. Struct.*, **140**, 758-775.
Yan, Z. and Jiang, L.Y. (2011), "The vibrational and buckling behaviors of piezoelectric nanobeams with surface effects", *Nanotechnol.*, **22**(24), 245703.
Yan, Z. and Jiang, L.Y. (2012), *Vibration and Buckling Analysis of a Piezoelectric Nanoplate Considering Surface Effects and In-Plane Constraints*, Proc. R. Soc. A, The Royal Society.
Yang, W., Liang, X. and Shen, S. (2015), "Electromechanical responses of piezoelectric nanoplates with flexoelectricity", *Acta Mech.*, **226**(9), 3097-3110.
Zang, J., Fang, B., Zhang, Y.W., Yang, T.Z. and Li, D.H. (2014), "Longitudinal wave propagation in a piezoelectric nanoplate considering surface effects and nonlocal elasticity theory", *Phys. E: Low-Dimens. Syst. Nanostruct.*, **63**, 147-150.
Zhang, C., Chen, W. and Zhang, C. (2013), "Two-dimensional theory of piezoelectric plates considering surface effect", *Eur. J. Mech.-A/Sol.*, **41**, 50-57.
Zhang, J., Wang, C. and Chen, W. (2014b), "Surface and piezoelectric effects on the buckling of piezoelectric nanofilms due to mechanical loads", *Meccan.*, **49**(1), 181-189.
Zhang, L.L., Liu, J.X., Fang, X.Q. and Nie, G.Q. (2014a), "Size-dependent dispersion characteristics in piezoelectric nanoplates with surface effects", *Phys. E: Low-Dimens. Syst. Nanostruct.*, **57**, 169-174.
Zhang, Z. and Jiang, L. (2014), "Size effects on electromechanical coupling fields of a bending piezoelectric nanoplate due to surface effects and flexoelectricity", *J. Appl. Phys.*, **116**(13), 134308.
Zhang, Z., Yan, Z. and Jiang, L. (2014), "Flexoelectric effect on the electroelastic responses and vibrational behaviors of a piezoelectric nanoplate", *J. Appl. Phys.*, **116**(1), 014307.

CC